Nano Research
2020, 13(9): 2313–2322

ISSN 1998-0124 CN 11-5974/O4
https://doi.org/10.1007/s12274-020-2880-z

Recent progress for hydrogen production by photocatalytic natural or simulated seawater splitting

Jining Zhang[1,2], Wenping Hu[2], Shuang Cao[1] (✉), and Lingyu Piao[1,3] (✉)

[1] *CAS Center for Excellence in Nanoscience, CAS Key Laboratory of Standardization and Measurement for Nanotechnology, National Center for Nanoscience and Technology, Beijing 100190, China*
[2] *School of Science, Tianjin University, Tianjin 300072, China*
[3] *Center of Materials Science and Optoelectronics Engineering, University of Chinese Academy of Sciences, China*

Received: 25 March 2020 / **Revised:** 6 May 2020 / **Accepted:** 17 May 2020

ABSTRACT

Solar energy is an inexhaustible renewable energy source. Among the various methods for solar energy conversion, photocatalytic hydrogen (H_2) production is considered as one of the most promising ways. Since Fujishima pioneered this field in 1972, photocatalytic water splitting to produce H_2 has received widespread attention. Up to now, abundant semiconductor materials have been explored as photocatalysts for pure water splitting to produce H_2. However, photocatalytic seawater splitting is more in line with the concept of sustainable development, which can greatly alleviate the problem of limited freshwater resource. At present, only few studies have focused on the process of H_2 production by photocatalytic seawater splitting due to the complex composition of seawater and lack of suitable photocatalysts. In this review, we outline the most recent advances in photocatalytic seawater splitting. In particular, we introduce the H_2 production photocatalysts, underlying mechanism of ions in seawater on photocatalytic seawater splitting, current challenges and future potential advances for this exciting field.

KEYWORDS

photocatalytic, seawater, hydrogen production, photocatalytic mechanism

1 Introduction

With the gradual exhaustion of fossil energy and the environment pollution, exploiting clean renewable energy is already in the extremely urgency [1, 2]. Development and utilization of sustainable and clean energy sources become a significant way to solve the energy and environmental dilemma [3–8]. The solar energy is one kind of inexhaustible and natural regeneration sources [9]. Therefore, the effective conversion of solar energy into hydrogen energy is considered as one of the most promising methods to solve energy and environment issues and has attracted much attention [10]. The energy content of H_2 is about 122 $kJ \cdot g^{-1}$, which is much higher than that of hydrocarbons. Besides, when hydrogen fuel is used to generate electricity, water is the only product. So, hydrogen energy is considered to be the promising environmental friendly energy [11–14]. Solar-driven water splitting into hydrogen energy is an irresistible trend [15–19].

With the rapid population growth, water crisis has sounded warning because of co-existence of serious water pollution and waste all over the world [20]. Especially, freshwater that can be directly utilized by mankind, should be protected and developed rationally in order to achieve sustainable development of water resource [21–23]. Seawater is the most abundant natural resource on earth, about 97% of the water is seawater, and the potential of seawater splitting into H_2 is extremely huge [24, 25]. Since the preliminary work in 1997 [26], more than 30 research groups have carried out the related research of photocatalytic seawater splitting. Seawater is rich in inorganic salts (NaCl, $MgCl_2$, etc.), organic matter and microorganisms [27]. Owing to the high salinity, the dissolved salts in seawater may deactivate catalysts or consume the photogenerated carriers and lead to undesirable side reactions [28]. As a result, the activity and durability of the photocatalysts are drastically compressed in seawater as compared to pure water [29]. However, every coin has two sides. Compared with the photocatalytic splitting pure water, the development of the photocatalytic seawater splitting has three significant advantages: (1) it can not only make full use of abundant seawater resource, solving the problem of lack of freshwater resource, but also greatly reduce the cost of the solar energy conversion process, which is more in line with actual application requirements [30]; (2) for some well-designed systems, the inorganic salts and other impurities can improve the performance of photocatalytic seawater splitting [25, 31]; (3) other high-value added by-products may be produced, such as ClO^- [32]. Although there have been some reports on electrocatalysis or photoelectrocatalysis [27], photocatalysis has the following advantages in comparison: (1) the use of solar energy is helpful for energy saving and environmental protection; (2) the reaction medium does not require the addition of additional electrolytes, reducing costs of product separation. Therefore, the development of highly efficient photocatalytic systems for H_2 production by seawater splitting is highly desirable. In this review, we highlight recent progress in photocatalytic seawater splitting, with the goal of providing inspiration to spur future advances in this important field.

Address correspondence to Shuang Cao, caos@nanoctr.cn; Lingyu Piao, piaoly@nanoctr.cn

2 Photocatalytic seawater splitting

2.1 Mechanisms of photocatalytic water splitting

The mechanism of photocatalytic water splitting is shown in Fig. 1(a). Under suitable light irradiation which has higher than or equal to the band gap of a semiconductor, the electrons and holes are generated on the conduction and valence band of the semiconductors, respectively [33, 34]. Under this suitable light irradiation, if the valence band of a semiconductor material is lower than the oxidation potential of H_2O (+1.23 V vs. SHE, pH = 0) and the conduction band is higher than the reduction potential of H_2O (0 V vs. SHE, pH = 0), water splitting reaction occurs and generates hydrogen and oxidation products [6, 8, 11, 35, 36]. To prevent the recombination of the photogenerated electrons and holes and improve surface reaction efficiency, loading appropriate co-catalysts on the surface of semiconductors is a wide accepted strategy [37, 38]. For seawater, photocatalytic processes are similar with pure water. However, the various salts and other component in seawater may influence the surface reaction and products [25, 39]. For example, oxidation potential of chloride ion is lower than that of H_2O, so oxidation products may contain chlorine [24, 39]. The redox potentials for the main components are shown in Fig. 1(b). Considering the NaCl is the dominant component, therefore, we mainly discuss the effect of Na^+ and Cl^- in seawater on photocatalytic seawater splitting later in this review.

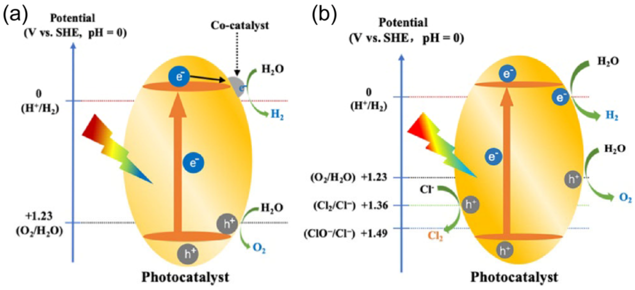

Figure 1 Typical energy band model of photocatalytic (a) pure water splitting, and (b) seawater splitting.

2.2 Photocatalyst system

Based on the reported works, we divided photocatalyst categories into TiO_2 series, g-C_3N_4 and other types of photocatalysts. To make a clear description, the relevant literatures are summarized into two tables (Tables 1 and 2) according to the factors affecting the photocatalytic activity, such as light

Table 1 Summary of photocatalytic seawater splitting systems based on titanium oxide materials

Photocatalyst	Seawater type	Light source	Sacrificial agent	Co-catalyst	H_2 production rate ($\mu mol\cdot h^{-1}\cdot g^{-1}$)	Efficiency	Stability	Performance better than pure water?	References
Nano TiO_2 (P25)	Simulated seawater (3% NaCl solution)	UV light (300 W Xe lamp)	—	CuO	3.1	—	—	No	[44]
Nano TiO_2 (P25)	Simulated seawater	UV light (300 W Xe lamp)	Oxalic acid	CuO	1.7	—	—	No	[46]
SiO_2/Ag @ TiO_2 core–shell	Simulated seawater	UV light ($35.3\ mW\cdot cm^{-2}$, 365 nm) full spectrum ($100\ mW\cdot cm^{-2}$, 300 W Xe lamp)	Glycerol	—	UV light：370 full spectrum 857	—	2 h × 5 cycle	—	[43]
Nano TiO_2 (P25)	Seawater (not specified)	Concentrated sunlight	Cyclohexane	—	1×10^5	—	—	Yes	[47]
Ti^{3+} self-doping Ti-O-Si	Simulated seawater (5% NaCl solution)	Sunlight	TEOA[a]	—	1,640	AQE[b]: 8.9%	—	Yes	[48]
CdS/TiO_2 nanocomposite material	Artificial seawater (3.5‰ salinity)	Visible light (450 W Hg lamp)	Na_2S, Na_2SO_3	Pt	2,640	—	—	Yes	[27]
CdS/TiO_2 composite material	Simulated seawater	Visible light (250 W high Hg lamp)	Na_2S, Na_2SO_3	Pt	457	—	Stable H_2 release after 20 h of light	Yes	[43]
Porous brookite TiO_2 nanoflutes	Seawater (not specified)	UV light (500 W Hg lamp) Natural sunlight	—	Pt	UV light: 7,200 Natural sunlight: 3,600	43.4% (λ > 300 nm)	more than 10 days (12 h/day, average rate ~ 2.0 $\mu mol\cdot h^{-1}\cdot mg^{-1}$)	No	[50]
TiO_{2-x} doped by H	Natural seawater (pH ~ 8.5)	AM 1.5[c]	Methanol	Pt	6,310	—	—	No	[51]
TiO_2 granules	Seawater (not specified)	λ > 320 nm ($558\ mW\cdot cm^{-2}$)	Glycerol	Pt	1,533	—	—	No	[52]

[a] Triethanolamine; [b] apparent quantum efficiency; [c] air mass 1.5 (1.5: solar spectrum obtained from zenith angle ≈ 48.2°, light intensity: $100\ mW\cdot cm^{-2}$).

Table 2 Summary of photocatalytic seawater splitting systems by other types of photocatalysts

Photocatalyst	Seawater type	Light source	Sacrificial agent	Co-catalyst	H_2 production rate (μmol·h^{-1}·g^{-1})	Efficiency	Stability	Performance better than pure water?	References
p-GaN/InGaN	Simulated seawater	AM 1.5	—	Rh/Cr_2O_3, cobalt oxide	5.1×10^6	STH 1.9% (27 sun intensities) AQE: 12.2% ($\lambda < 400$ nm)	—	Yes	[39]
$La_2Ti_2O_7$	Natural seawater	UV light (400 W Hg lamp)	—	NiO, Ni	696	—	—	No	[27]
(Ni-ZnO)@C core–shell nanoreactor	Simulated seawater	UV light (300 W Xe lamp)	Methanol	—	5.01	—	—	—	[56]
WO_2-Na_xWO_3 hybrid conductor materials	Seawater (pH = 6.5)	Solar spectrum (1,000 W Xe lamp)	—	—	5.76	STH: 0.25 (Xe lamp irradiation)	—	Yes	[57]
$Cd_xZn_{1-x}Se$	Simulated seawater	AM 1.5	Na_2S, Na_2SO_3	CoP	36,600	—	7 h	No	[58]
$ZnS_{1-x-0.5y}O_x(OH)_y$-ZnO	Simulated seawater	Visible light (400 W Hg lamp)	Na_2S, Na_2SO_3	—	183	—	12 h	Yes	[29]
$ZnS_{1-x-0.5y}O_x(OH)_y$-ZnO	Simulated seawater	Visible light (400 W Hg lamp)	Na_2S, Na_2SO_3	NiS	354	—	—	Yes	[30]
Organic conjugated molecules PorFN	Simulated seawater	AM 1.5	TEOA	Pt	10,900	—	—	Yes	[59]
Covalent organic polymer COP-$TP_{x:y}$	Simulated seawater	Visible light (300 W Xe lamp)	TEOA	Pt	4,250	AQE: 1.5% ($\lambda = 400$ nm)	Discontinuous irradiation activity decreased by 7% within 1 month	No	[60]
Thioether-functionalized covalent organic framework	Seawater (not specified)	Visible light (300 W Xe lamp)	TEOA	Au	125	—	20 h	No	[28]
Conjugated covalent organic polymer	Seawater (not specified)	Visible light (300 W Xe lamp)	Na_2S, Na_2SO_3	Carbon-encapsulated nickel phosphide	2,500	AQE 2.5% ($\lambda = 400$)	Maintains 92% of initial efficiency after 16 intermittent cycles which lasts for half a month	No	[61]
CdS nanosheets	Natural seawater from China Yellow Sea	Visible light (300 W Xe lamp)	Lactic acid	Carbon dots (CDs)	4,640	AQE: 11.8% ($\lambda = 420$ nm)	—	No	[62]
$(Ga_{1-x}Zn_x)(N_{1-x}O_x)$	Simulated seawater (pH = 8.0)	Visible light (450 W Hg lamp)	—	$Rh_{2-y}Cr_yO_3$	333	—	—	No	[64]

source, sacrificial agents, co-catalysts and catalytic performance.

2.2.1 *Titanium oxide photocatalysts*

Due to the merits of good stability, low cost, and non-toxicity, titanium dioxide-based photocatalysts have attracted sustained attention in various research fields [40, 41]. The most widely used photocatalyst in the field of photocatalytic seawater splitting is still titanium dioxide-based photocatalysts. The relevant articles are summarized in Table 1.

All the mentioned photocatalysts above are based on micro-nano titanium oxide materials with some of them being modified by CdS [27, 42], Ag and so on [43]. The reaction media is mainly simulated seawater which was prepared accounting to salinity of natural seawater (NaCl, 27.21 g; $MgCl_2$, 3.81 g; $MgSO_4$, 1.66 g; $CaSO_4$, 1.404 g; K_2SO_4, 0.577 g; K_2CO_3, 0.2124 g; $MgBr_2$, 0.08 g were dissolved in 1 L distilled water) or NaCl solution [27, 44]. Meanwhile, there are also articles that use natural seawater as a reaction medium [27, 45]. The composition of natural seawater is not only complicated, but the presence of solid particles and microorganisms also increases the difficulty of studying photocatalytic seawater splitting. Therefore, it is recommended to use simulated seawater with quantitative composition as the solution for an initial research [39].

2.2.1.1 Light source

The ideal light source for photocatalytic seawater splitting is sunlight. Among the titanium oxide systems, three kinds of light sources including sunlight, ultraviolet (UV) light and visible light, have been introduced. When the sacrificial agents and co-catalysts are similar, the performance of titanium oxide-based photocatalysts under sunlight and UV light is better than that of under visible light irradiation, which is directly related to its wide bandgap. Simamora et al. introduced TiO_2 as a photocatalyst for seawater splitting under UV light in 2012 and 2013 with the H_2 evolution rates of 3.1 and 1.7 $\mu mol\cdot h^{-1}\cdot g^{-1}$, respectively [44, 46]. As a co-catalyst, CuO can expand the absorption wavelength of TiO_2 to visible light, which can increase the performance photocatalytic seawater splitting in this article [44]. Both of them were lower than that of in pure water (5.0 and 8.48 $\mu mol\cdot h^{-1}\cdot g^{-1}$, respectively). Gao et al. reported that the H_2 evolution rate of photocatalytic seawater splitting by core–shell material ($SiO_2/Ag@TiO_2$) was 370 $\mu mol\cdot h^{-1}\cdot g^{-1}$ under UV light irradiation [43]. Visible and ultraviolet light in sunlight can be absorbed by the core and shell structures, respectively. With regard to the selection of light sources, we suggest that it is appropriate to adapt the light absorption properties of the photocatalyst and try to use sunlight as the light source to meet the actual needs.

2.2.1.2 Sacrificial agents and co-catalysts

In the field of photocatalytic pure water splitting, many studies have achieved overall water splitting and no longer using sacrificial agents which acts as electron donor or acceptor and accelerates the separation of photogenerated electrons and holes [6]. However, most of the titanium oxide systems still use sacrificial agents to achieve the semi-reactive seawater splitting, which is necessary for the study of the initial mechanism of H_2 production from seawater splitting. Notably, from another perspective, the large amount of inorganic and organic substances in seawater can play the role of sacrificial agent itself to improve the photocatalytic performance, which is valuable for practical application.

The use of co-catalysts will greatly affect the H_2 evolution rate of photocatalytic seawater splitting. There are three works in Table1 that did not use co-catalysts [43, 47, 48], and two works used CuO to replace the noble metal Pt co-catalysts with a dramatically decreased H_2 evolution rate [44, 46]. However, the use of the noble-metal-free co-catalysts indicates that the researchers have paid more attention to use non-noble metal co-catalysts or no co-catalyst as further research direction to meet the needs of practical applications.

2.2.1.3 Performance

Most of the research results in Table 1 show that the performance of H_2 production in seawater is higher than that of in pure water under the same conditions. For titanium oxide photocatalysts, the performances had a large difference for different systems, with the H_2 evolution rates distributing from 1.7 to 1×10^5 $\mu mol\cdot g^{-1}\cdot h^{-1}$. However, it is not significant to interpret the performance difference simply, which needs to be analyzed in combination with different experimental conditions.

Deepan Prakash et al. introduced nano-TiO_2 (P25) as a photocatalyst and cyclohexane as a sacrificial agent to evaluate the photocatalytic seawater splitting performance under a concentrated light irradiation [47]. Concentrated light was the sunlight collected and concentrated by concentrating systems which used lenses or reflectors [49]. The H_2 evolution rate reached up to 1×10^5 $\mu mol\cdot g^{-1}\cdot h^{-1}$. Under the same condition, the H_2 evolution rate of photocatalytic pure water splitting was only half of that value (5×10^4 $\mu mol\cdot g^{-1}\cdot h^{-1}$). The author thought that solar concentrator played an important role in the high H_2 evolution rate. At the same time, the presence of electron-donating groups such as sodium ions in the seawater attributed to the higher H_2 evolution rate in seawater than that of in pure water. In this system, the photocatalytic processes of photo-generated electrons and holes are shown in Eqs. (1) and (2), respectively, and then the generated O_2 would react with cyclohexane to form ketones and enols as shown in Eq. (3). These two compounds are good electron donors and can continue to provide electrons for H^+ reduction, thus enhancing the H_2 evolution rate of photocatalytic seawater splitting.

$$e^- + H^+ \rightarrow 1/2H_2 \tag{1}$$

$$H^+ + OH^- \rightarrow 1/2O_2 + H^+ \tag{2}$$

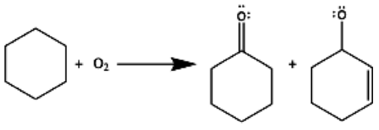

(3)

In 2019, Cao et al. reported a photocatalytic system which used porous brookite TiO_2 nanoflutes as photocatalyst and Pt as co-catalyst. Under UV light and natural light irradiation, the H_2 production rates of photocatalytic seawater splitting were 7,200 and 3,600 $\mu mol\cdot g^{-1}\cdot h^{-1}$, respectively, which is the highest value among the reported works without using any sacrificial agents [50]. The excellent performance may be due to the high crystallinity, special surface properties of the obtained single crystal brookite TiO_2 nanoflutes.

Song et al. reported a Ti^{3+} (oxygen vacancy) self-doped titanium-silicon material (Ti–O–Si), which can resist the corrosion of Ti in seawater [48]. Under full sunlight, the H_2 evolution rate of Ti-O-S (1930.5 $\mu mol\cdot h^{-1}\cdot g^{-1}$) is 43.1 times higher than that of pure phase TiO_2 (44.8 $\mu mol\cdot h^{-1}\cdot g^{-1}$) in simulated seawater (5% NaCl solution) with TEOA as the sacrificial agent. In pure water, the efficiency is 10-fold higher for Ti–O–Si (1,640.2 $\mu mol\cdot h^{-1}\cdot g^{-1}$) than that of pure TiO_2 (163.2 $\mu mol\cdot h^{-1}\cdot g^{-1}$). Under visible light irradiation (420 nm), the AQE in simulated seawater (5% NaCl solution) was 8.9%. Figure 2(a) shows the comparison of H_2 evolution efficiencies for different samples prepared at different calcination temperatures, and Fig. 2(b) is the energy level diagram and molecular structure of the Ti–O–Si (400).

The highlight of the research by Gao et al. is photothermal synergy effect in the photocatalytic seawater splitting reaction [43]. The $SiO_2/Ag@$ TiO_2 is a core-shell structure material with TiO_2 being coated by SiO_2 spheres. As shown in Fig. 3, Ag nanoparticles are embedded in SiO_2 spheres. Due to the characteristics of the core-shell structure, the TiO_2 shell can use the ultraviolet light in sunlight, and the SiO_2/Ag core can use low-energy photons to generate thermal effects that are useful for the photocatalytic reaction. The photothermal effect of the material can directly induce surface catalysis by heating and subsequently promote H_2 production from seawater. Under the full spectrum irradiation, the H_2 evolution rate from natural seawater was 857 $\mu mol\cdot g^{-1}\cdot h^{-1}$. After five cycles' reaction (2 h/cycle), the H_2 evolution rate fluctuated within the range of 7%.

Ji and Peng et al. used CdS/TiO_2 composite material as photocatalyst, Pt as co-catalyst, and Na_2S and Na_2SO_3 as sacrificial agents for H_2 production by photocatalytic seawater splitting in 2007 and 2013, respectively [27, 42]. However, the performance of these two systems varies greatly. Under visible light, Ji et al. got the H_2 evolution rates of 1,860, 1,950, 2,640 and 1,660 $\mu mol\cdot h^{-1}\cdot g^{-1}$ in natural seawater, artificial seawater

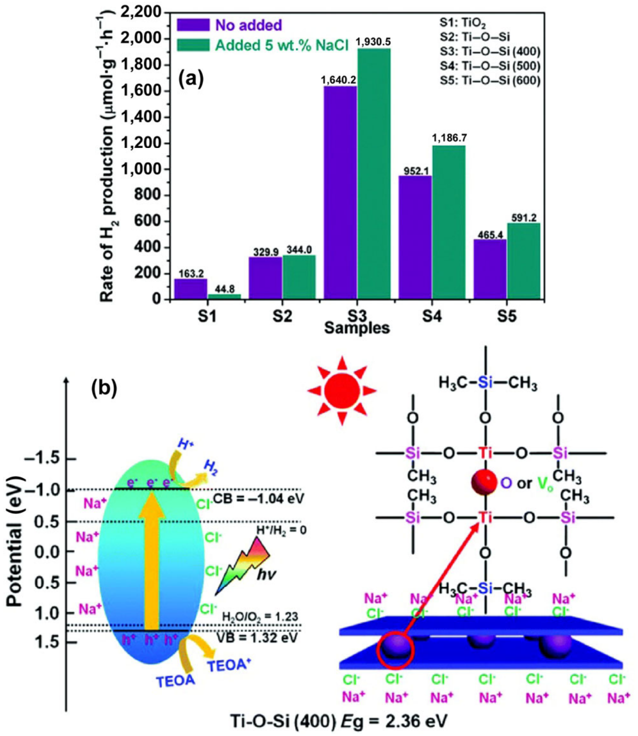

Figure 2 (a) H_2 evolution rate of Ti–O–Si prepared at different calcination temperatures. (b) Possible mechanism of Ti-O-Si (400) photocatalytic artificial seawater splitting. Reproduced with permission from Ref. [48], © The Royal Society of Chemistry 2018.

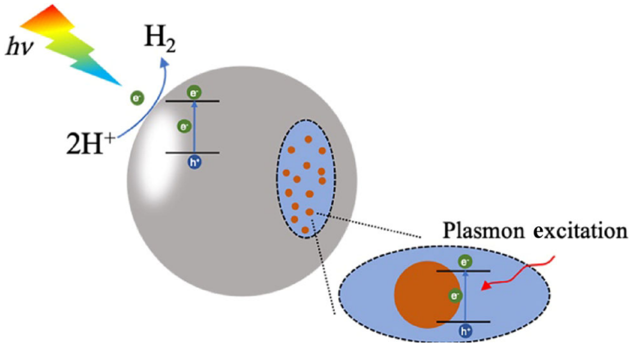

Figure 3 The table of contents for $SiO_2/Ag@TiO_2$ system.

with salinity of 17.5‰, 3.5‰, and pure water, respectively. However, the photocatalyst was inactive without sacrificial agents, therefore, it can be seen that the function of this photocatalyst depends on the presence of sacrificial agent. The CdS/TiO_2 composite material reported by Peng et al. demonstrated the H_2 evolution rates of 456.6 and 306.3 μmol·h⁻¹·g⁻¹ in seawater and pure water, respectively, under the same conditions. The difference in activity is related to the category and concentrations of sacrifices agents used. Compared with the concentration of sacrificial agents used by Ji et al. (0.01 mol·L⁻¹ Na_2S and 0.002 mol·L⁻¹ Na_2SO_3), a much more high concentration (0.1 mol·L⁻¹ Na_2S and 0.1 mol·L⁻¹ Na_2SO_3) was introduced by Peng et al., which caused an imbalance in the charge of seawater and hindered its function as a sacrificial agent.

In 2018, Sinhamahapatra and Sakurai et al. reported using hydrogenated TiO_2 and powdered TiO_2 particles as photocatalysts, methanol and glycerol as sacrificial agents, respectively, Pt as a co-catalyst. The rates of H_2 evolution of photocatalytic seawater splitting were lower than that of in pure water under irradiation of AM 1.5, which is different from the above study, the authors infer that it may be caused by other substances in seawater, such as adsorption inhibition of electrolyte layer formation, electron acceptor effect of Cl^- or precipitation formed by Mg^{2+} and OH^- [45, 51]. When shaking the seawater reactor, the H_2 evolution rate increased significantly, indicating that the main reason for the decrease in seawater activity was flocculation of photocatalyst particles [51].

Only very few studies provide both efficiency and stability. Based on the limited reported works, it can be indicated that the stability in seawater is lower than that in pure water.

2.2.2 *g-C₃N₄ photocatalysts*

$g-C_3N_4$ has been widely studied and applied to various photocatalytic systems. Among the retrieved articles on H_2 production by photocatalytic seawater splitting by using $g-C_3N_4$ as photocatalyst, there are only three works. Speltini et al. and Yang et al. used oxidized $g-C_3N_4$ ($o-g-C_3N_4$) and $WS_2/C-TiO_2$ nanorod modified $g-C_3N_4$ as photocatalyst, respectively, Pt as co-catalyst under visible light irradiation [52, 53]. For both of the systems, the H_2 evolution rate in seawater is higher than that of in pure water. In the work by Speltini et al., the H_2 evolution rates in natural seawater were 2,523 and 847 μmol·h⁻¹·g⁻¹ under natural and simulated sunlight (500 mW·cm⁻²) irradiation, respectively, using glucose as a sacrificial agent. By contrast, the H_2 evolution rate in deionized water splitting was 840 μmol·h⁻¹·g⁻¹. Yang et al. used TEOA as sacrificial agent. The H_2 evolution rates were 1,199.12 and 709.04 μmol·h⁻¹·g⁻¹, in natural seawater and pure water, respectively, under visible light irradiation, the authors thought that Cl^- in seawater can be oxidized by photogenerated holes and promote the separation of photogenerated charges, that is, it acted as a sacrificial agent. The solar to hydrogen conversion efficiency (STH) was 2.04%. In this work, WS_2, $C-TiO_2$ and $g-C_3N_4$ can form a triple heterojunction, which shortened the charge transfer distance, accelerated the separation of photogenerated charges, and enhanced photocatalytic activity. The energy level of the composite material is shown in Fig. 4. Because the conduction band potential of $g-C_3N_4$ is lower than the other two components, the photogenerated electrons in the conduction band of WS_2 and $C-TiO_2$ are transferred to $g-C_3N_4$. In contrast, the holes generated by $g-C_3N_4$ are injected into the valence bands of WS_2 and $C-TiO_2$. The opposite migration paths of photogenerated electrons and holes in the composite material greatly promote charge separation and enhance the photocatalytic activity of photocatalytic seawater splitting. Although composite material in Yang's work possesses a well-designed structure

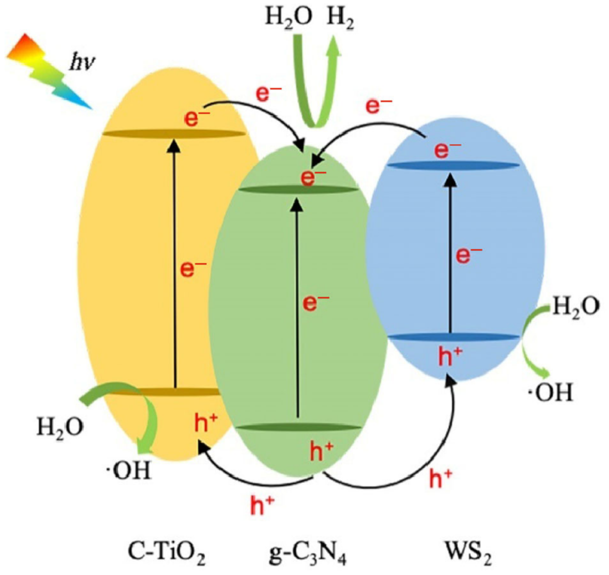

Figure 4 Photocatalytic energy level diagram of the composite material.

that can improve the photocatalytic efficiency, such as heterojunction, the rate of H_2 evolution under visible light was still lower than that of oxidized g-C_3N_4 described above under sunlight due to the difference of sacrificial agents.

In 2019, Chaudhary et al. reported that mesoporous g-C_3N_4 with the nitrogen deficiency as photocatalyst, tert-butylpyridinecobaloxime as co-catalyst and TEOA as sacrificial agent for seawater splitting [54]. Because of the mesoporous structure with enlarged surface area and nitrogen deficiency, the photogenerated charge separation can be effectively promoted and electron-hole recombination can be greatly restrained. Under optimized conditions, the H_2 evolution rate in natural seawater reached up to 33,333 $\mu mol\cdot h^{-1}\cdot g^{-1}$ with the AQE value of 4% under visible light irradiation. The photostability of H_2 production could sustain for 20 h.

g-C_3N_4 has a band gap (2.7 eV) which is narrower than that of TiO_2 (3.2 eV), so wavelengths of light that g-C_3N_4 can absorb are longer than that of TiO_2 can absorb. In addition, mesh structure provides more active sites which can increase carrier separation efficiency. From the perspective of H_2 evolution efficiency, the H_2 evolution rate of g-C_3N_4 is higher than that of titanium oxide, but the numbers of studies of photocatalytic seawater splitting to produce H_2 using g-C_3N_4 is fewer than that of TiO_2, so the research progress of g-C_3N_4 should be further developed.

2.2.3 *Other types of photocatalysts*

Other photocatalysts are heterogeneous and do not form a single system. They are summarized in Table 2.

For the other types of photocatalysts, inorganic materials are the majority, such as mixed materials doped with CdS and other substances. There is also no shortage of organic photocatalysts, such as organic conjugated molecules and covalent organic polymers. The seawater used is mainly simulated seawater, which is helpful for the qualitative and quantitative study of the effects of different components in seawater on the photocatalytic process. Because the types are not uniform, and the conditions of the respective systems are not the same, the level of H_2 evolution rate is only used as one of evaluation parameter, and there is no meaningless to evaluate which is better.

2.2.3.1 Light source

At present, researchers tend to use sunlight or visible light as a light source, which means that they are making a constant effort to achieve the ultimate target of direct converting solar energy into chemical energy. Similar to titanium oxide photocatalysts, there are two articles using UV light as a light source for photocatalytic seawater splitting to satisfy its bandgap. In 2007, Ji et al. reported the system using NiO and Ni loaded $La_2Ti_2O_7$ as photocatalyst [27], which has a wide band gap (3.8 eV) and can only absorb UV light [55]. The H_2 evolution rate reached to 696, 598, and 1,372 $\mu mol\cdot h^{-1}\cdot g^{-1}$ in natural seawater, simulated seawater and pure water, respectively. It indicated that the H_2 evolution rate in seawater was lower than that in pure water and authors thought that Mg^{2+} is the main reason for reducing the rate of hydrogen evolution compared to other ions. In 2014, Yang et al. reported the (Ni-ZnO)@C shell core nanoreactor, in which Ni and ZnO were embedded in C [56]. Under UV light irradiation, the H_2 evolution rate of photocatalytic simulated seawater splitting was 5.01 $\mu mol\cdot h^{-1}\cdot g^{-1}$ using methanol as the sacrificial agent.

2.2.3.2 Sacrificial agents and co-catalysts

Most of the reported works have introduced both sacrificial agents and co-catalysts to achieve high H_2 production efficiency, and only the mixed semiconductor material WO_2-Na_xWO_3 reported by Cui et al. did not use sacrificial agent and co-catalyst [57]. Common sacrificial agents of Na_2S and Na_2SO_3 appeared in three articles [29, 30, 58], and other works used readily available organic reagents such as methanol, lactic acid and TEOA to increase the H_2 evolution rate. Precious metal Pt or Au nanoparticles are chosen as a highly effective co-catalysts in three works [28, 59, 60]. Most of the other articles introduced transition metal oxides as co-catalysts, which suggested that researchers are making effort to reduce the cost.

In 2011, Li et al. developed a $ZnS_{1-x-0.5y}O_x(OH)_y$-ZnO photocatalyst driven by visible light to achieve H_2 production by introducing Na_2S and Na_2SO_3 as sacrificial agents in simulated seawater [29]. A H_2 evolution rate of 183 $\mu mol\cdot h^{-1}\cdot g^{-1}$ was achieved and could sustain for more than 12 h. Then, the author further found that the inorganic salt ions in seawater would react with Na_2S and Na_2SO_3 to form $Mg(OH)_2$ and $CaSO_3$ precipitates, which covered the active sites of the photocatalyst and further reduced the light absorption of the photocatalyst [30]. However, when NiS was supported on the surface of $ZnS_{1-x-0.5y}O_x(OH)_y$-ZnO as co-catalyst, the negative charge on the photocatalyst surface could be increased. Due to electrostatic repulsion, it would be difficult to form the negatively charged precipitates on the surface of the photocatalyst. Therefore, using NiS as co-catalyst, the H_2 evolution rate of photocatalytic seawater splitting under visible light could reach up to 354 $\mu mol\cdot h^{-1}\cdot g^{-1}$. The energy level diagram of the photocatalyst is shown in Fig. 5.

In 2019, Li et al. reported a photocatalyst which had a thioether-functionalized 2D covalent organic framework (COF) [28]. In this work, Au and TEOA were used as co-catalyst and sacrificial agent, respectively. It is proposed that the plasmonic effects of Au promoted the separation of photogenerated carriers. Besides, the large surface area of COF provided more active sites and promoted mass transfer process.

Liu et al. reported a conjugated covalent organic polymer as photocatalyst, Na_2SO_3 and Na_2S as sacrificial agents [61]. Authors used carbon-encapsulated nickel phosphide(CNi$_2$P) as co-catalyst which is noble-metal-free. Under visible light irradiation, the H_2 production rate from seawater was 2,500 with the AQE value of 2.5%.

2.2.3.3 Performance

Similar to titanium oxide photocatalysts, the H_2 evolution rate for other types of photocatalysts also has relatively wide

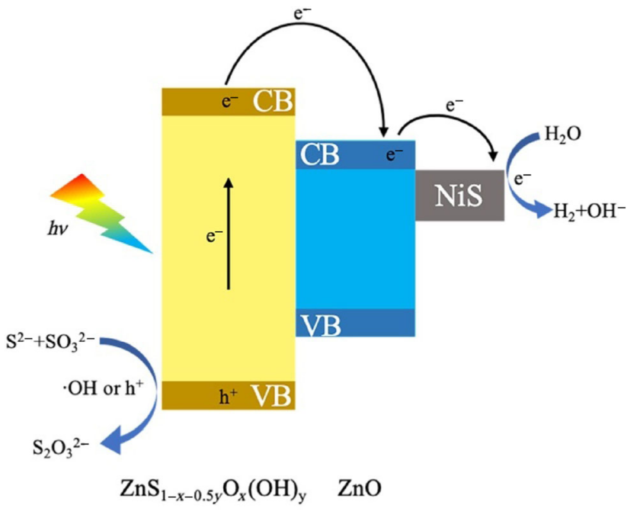

Figure 5 Energy level mechanism diagram of photocatalyst.

distribution interval: 5.01 to 5.1 × 10^6 μmol·h^{-1}·g^{-1}, due to the different experimental conditions. Here, we main talk about the top five photocatalysts for H_2 production.

First of all, the highest H_2 evolution rate was reported by Guan et al. in 2018 [39]. The GaN nanowire cluster embedded with p-type InGaN (p-GaN/InGaN) was used as photocatalyst. Under sunlight irradiation, the H_2 evolution rates in simulated seawater and pure water were 5.10 × 10^6 and 4.84 × 10^6 μmol·h^{-1}·g^{-1}, respectively, using Rh/Cr_2O_3 and cobalt oxide as co-catalysts and without using any sacrificial agent. It is worth noting that under 27 solar light irradiation, the STH and AQE values achieved 1.9% and 12.2%, respectively. Although no sacrificial agent was used, the design of multicomponent structure significantly increased the H_2 evolution rate. At the same time, it also should be noted that the photocatalyst preparation process in this system is complicated and developing simple and robust photocatalysts is still the direction of effort.

The second highest H_2 evolution rate is achieved by the CdZnSe system. Qiu et al. reported the $Cd_{0.25}Zn_{0.75}Se$ photocatalyst in 2016 [58]. Under simulated sunlight irradiation, the H_2 evolution rate was 36,600 μmol·h^{-1}·g^{-1}, 5.0% CoP was used as co-catalyst, 1.25 mol·L^{-1} Na_2S and 1.75 mol·L^{-1} Na_2SO_3 as sacrificial agents in artificial seawater. By contrast, the H_2 production efficiency in pure water was 45,000 μmol·h^{-1}·g^{-1}. Due to the appropriate Cd doping concentration and suitable conduction band position, the H_2 production efficiency and stability could be optimized apparently. After 7 hours of irradiation, the photocatalyst still demonstrated robust H_2 evolution performance.

In 2019, Yang et al. developed a small positively charged molecule PorFN based on a zinc-porphyrin core (Fig. 6(a)) with the H_2 evolution performance locating at the third place [59]. Due to the electrostatic interaction between Cl^- and positively-charged PorFN molecules, the high concentration of Cl^- could promote large-scale aggregation of PorFN. The self-assembly formed "superstructure" could not only promote charge transfer, but also improve the photocatalytic efficiency. The H_2 evolution rate was 200 μmol·h^{-1}·g^{-1} in pure water. In 0.50 M NaCl solution, the H_2 production rate increased significantly to 10,900 μmol·h^{-1}·g^{-1}. In the neutral solution, the redox potential of Cl^- (+0.98 V vs. NHE, pH = 7) is lower than the valence band of PorFN (+0.76 V vs. NHE), therefore, the Cl^- would not act as a hole scavenger in this system and the role of Cl^- in the system was only to promote the self-assembly of PorFN as shown in Fig. 6(b).

Almost at the same time, Zhu et al. reported that the carbon dot modified CdS photocatalyst (CDs/CdS) and its H_2 evolution performance located at the fourth place [62]. The H_2 evolution rates were 4,640 and 6,700 μmol·h^{-1}·g^{-1} in seawater and pure water, respectively, with the AQE value of 11.8% and 19.3%, respectively. The H_2 evolution rate of CDs/CdS was much higher than that of CdS photocatalyst alone, which is largely due to the fact that CDs act as good electron acceptors with excellent electron storage and transfer properties.

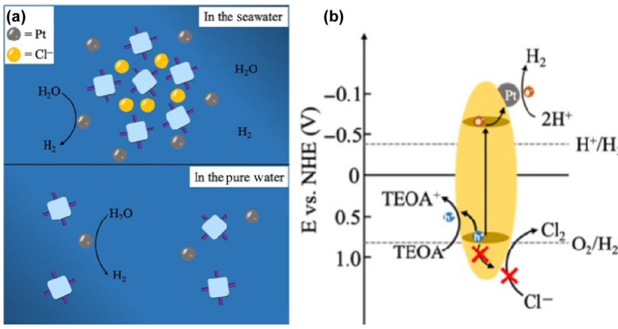

Figure 6 (a) PorFN chemical structure and proposed "superstructure" schematic diagram. (b) Energy level diagram of ProFN.

Due to the rapid charge transfer property of conjugation of benzene rings, Liu et al. used a co-construction of 1, 3, 6, 8-tetrabromopentadiene (TBP) and 3, 8-dibromophenanthroline (DBP) covalent organic polymer COP-$TP_{x:y}$ as a photocatalyst, the H_2 evolution rate ranked fifth [47]. Under visible light irradiation, the photocatalytic H_2 evolution rate from seawater was about 4,250 μmol·h^{-1}·g^{-1}. The highest AQE was 1.5% at 400 nm. The activity only decreased by 7% under discontinuous irradiation for one month, indicating the excellent stability of COP-$TP_{3:1}$.

2.3 The effect of ions on photocatalytic seawater splitting

Considering that the mechanism of photocatalytic pure water has been relatively mature, we believe that the mechanism of ions in seawater on photocatalytic seawater splitting should be studied on the basis of photocatalytic pure water. However, the mechanism of ions in seawater is still in the exploratory stage and need to be further studied. Up to now, there is no universal mechanism for different systems. Except water, the main component of seawater is NaCl and the reported articles mainly discussed the effects of Na^+ and Cl^- on the photocatalytic performance, therefore, it is necessary that we mainly discuss the effects of Na^+ and Cl^- in this review.

2.3.1 *Effects of Na^+*

Li et al. studied the effect of NaCl on the photocatalytic water splitting in the case of Pt/TiO_2 as photocatalyst and formic acid, oxalic acid, and ethanol as sacrificial agents, respectively [63]. The results indicated that under alkaline or neutral conditions, abundant Na^+ adsorbed on the surface of TiO_2 leading to the promotion adsorption of sacrificial agents on the surface of TiO_2. In this way, the sacrificial agents can easily combine with the photogenerated holes and facilitate charge separation and reduce electron-hole recombination. Peng et al. demonstrated that the content of ·OH had a close relationship with the photocatalytic performance of TiO_2, since the sacrificial agent could directly react with the holes before the holes react with OH^- to form ·OH. In pure water, more ·OH was detected than that in seawater, therefore, the H_2 production efficiency is much higher in seawater [42]. Maeda et al. found that alkali metal or their cations could promote photocatalytic seawater splitting in $Rh_{2-y}Cr_yO_3/(Ga_{1-x}Zn_x)(N_{1-x}O_x)$ system [64]. It is believed that solutions containing Na^+, such as NaCl and Na_2SO_4, could promote the redox reaction on the photocatalyst surface and eliminate the negative effect of the surface defects, which act as electron-hole recombination centers. All of the above are the positive effects of Na^+ on the photocatalytic seawater splitting. However, Li et al. also found that at a high NaCl concentration (>1.0 mol·L^{-1}), the sacrificial agent (glucose) would be indirectly adsorbed on the photocatalyst surface with the assistance of Na^+, and then reduced the charge transfer efficiency between photocatalyst and glucose [66].

2.3.2 *Effects of Cl^-*

Researchers have two different perspectives on the effect of Cl^- on photocatalytic seawater splitting.

2.3.2.1 Negative view

First of all, the negative effects of Cl^- focus on two points in the reported articles. One point of view is that Cl^- affects the adsorption of reactant on the surface of photocatalyst. In 2001, Li et al. conducted the related study and found that the adsorption of Cl^- on TiO_2 surface was weak leading to a little effect during the photocatalytic process [66]. In 2011, Li et al. reported that Cl^- tended to adsorb on the surface of TiO_2 under acidic condition [63]. Afterwards, Krivec et al. found that Cl^- could be adsorbed on the surface of TiO_2 [67]. On the one hand, it prevented the target reactants from adsorbing on the surface of TiO_2, and on the other hand, it competed with the sacrificial agent for reactive sites, making the hole-trapping agent unable to capture holes quickly. As a result, the photo-generated electron-hole recombination rate increased and the photocatalytic activity reduced. Gao et al. also speculated that Cl^- competed with the reactant at the active site, and as a result, the adsorption of H^+ or the sacrificial agent is suppressed [43].

It is also believed that Cl^- can act as a reactant and hinder the water splitting reaction. Maeda et al. found that Cl^- would be oxidized by the holes generated by $Rh_{2-y}Cr_yO_3/(Ga_{1-x}Zn_x)(N_{1-x}O_x)$ on the valence band [64]. In the presence of Cl^-, the photocatalytic activity of water splitting was inhibited, and this phenomenon was more serious under acidic conditions than in neutral solution. Li et al. believed that although Cl^- could react with holes, it also participated the reduction reaction with electrons on the conduction band, as shown in Eqs. (4) and (5), thus decreasing the photocatalytic activity [63]. Gao et al. also speculated the reason why the H_2 evolution rate of photocatalytic seawater splitting was lower than that of pure water [43]. It may be due to that the Cl^- in seawater could react with holes and donate an electron to generate Cl·, which continued to compete with H^+ reduction reaction as shown in Eqs. (5) and (6). No other chlorine-containing compounds were detected during the reaction, and the Cl^- concentration remained the same, which was consistent with the speculation.

$$Cl^- + h^+ \rightarrow \bullet Cl \tag{4}$$

$$\bullet Cl + e^- \rightarrow Cl^- \tag{5}$$

$$Cl\bullet + Cl^- \rightarrow Cl\bullet_2^- \tag{6}$$

$$Cl\bullet_2^- + e^- \rightarrow 2Cl^- \tag{7}$$

In addition, Simamora et al. believed that many hydroxyl groups on the surface of TiO_2, such as $TiOH_2$ and TiOH, could react with Cl^- to form TiCl and reduce the photocatalytic activity of seawater splitting [46]. But in general, all of the above are only at the speculative stage, and no more experimental data to confirm the conclusion.

2.3.2.2 Positive view

Regarding the role of Cl^-, there are also neutral or positive viewpoint. Ji et al. believed that although the holes on the valence band of $La_2Ti_2O_7$ (2.714 eV) possess the ability to oxidize Cl^-, no decrease of Cl^- concentration was observed during the 6 h of photocatalytic reaction [27]. So, the authors believed that it is insufficient to drive the oxidation of Cl^- kinetically, and Cl^- would not be oxidized during the photocatalytic seawater splitting reaction. Guan et al. found that although the oxidation of Cl^- to Cl_2 (Cl_2/Cl^-, 1.36 V vs. NHE, pH = 0) is more difficult than the oxidation of H_2O to O_2 (O_2/H_2O, 1.23 V vs. NHE, pH = 0), the oxidation of Cl^- to Cl_2 is a two-electron redox process, and the kinetics are more favorable [39]. Therefore, after the oxidation of Cl^- to Cl_2, the oxidation reaction of water is promoted in the following ways

$$Cl_2 + H_2O \rightarrow H^+ + Cl^- + HClO \tag{8}$$

$$2HClO \rightarrow 2H^+ + 2Cl^- + O_2 \tag{9}$$

Li et al. also proposed that at low NaCl concentration (< 1.0 mol·L^{-1}), the salt effect could promote the adsorption of the sacrificial agent on the surface of photocatalyst [65]. They also take the view that the NaCl concentration affects the hydration layer on the photocatalyst surface and then change the amount of surface charge and influence the activity [29]. That is, NaCl affects the H_2 production process by changing the surface properties and the contact between the sacrificial agent and the photocatalyst. Yang et al. believed that holes could be consumed by participating in the Cl^- oxidation reaction, thereby reducing the electron-hole recombination rate [53].

In summary, there are two different conclusions about the effect of ions in seawater on H_2 production. One is that the H_2 production efficiency in seawater is higher than that in pure water, because inorganic salts play the role of sacrificial agents. On the contrary, the H_2 efficiency in seawater is lower than that in pure water, and the related research work is relatively less. The role of inorganic salts is mainly recognized as a sacrificial agent, at the same time, inorganic salt can also change the physical and chemical properties of the photocatalyst surface, affecting the final H_2 production efficiency.

3 Conclusion and outlook

Among the reported 26 articles about photocatalytic seawater splitting, TiO_2 was the most widely used material (10 articles). In general, the photocatalytic performance of titanium oxide photocatalysts was above the median level and most of them demonstrated a higher H_2 production efficiency in seawater than that in pure water. Among the studies, the use of sunlight as the light source has generally achieved better performance in photocatalytic seawater splitting, and the activity is lower when using UV or visible light as the light source. In the application of H_2 production by photocatalytic seawater splitting, the stability of the photocatalyst plays a significant role. However, only 10 reported articles give the stability evaluation of the photocatalyst, and the stability is just passable. For the effects of ions on the photocatalytic efficiency, it is generally believed that Na^+ has a positive effect on the photocatalytic seawater splitting, and it remains controversial about the understanding of Cl^-. Nevertheless, it should be noticed that all the effects strongly depend on the kinds of photocatalysts used.

The production of H_2 using seawater as raw source is one of the most ideal methods to solve the energy problem. The above discussion mainly summarized the existing examples of H_2 production by photocatalytic seawater splitting. The work in this field has been attracted increasing attention in recent years, and it still has great potential to explore and improve. Among the existing research, the use of natural light is lacking and most of the systems still introduced both co-catalysts and sacrificial agents to improve the photocatalytic performance. Besides, the conversion efficiency is still unsatisfactory and most works lack discussion on stability.

It is worth noting, although the H_2 production efficiencies are various when compare seawater and pure water systems, the H_2 evolution rate is still considerable in seawater. Regardless the comparison with pure water, it is necessary to utilize seawater, because the seawater does not involve resource shortage and cost issues. At present, the influence of ions in seawater on the photocatalyst has received widespread attention, laying a solid foundation for the mechanism of H_2 production by photocatalytic seawater splitting. Based on the existing research, it is proposed that two points should be paid more attention when design an efficient photocatalysts for H_2 production from seawater: (1) Stability. The material should resist the oxidation by Cl_2, ClO^- and so on. (2) It is desired that the material can effectively take advantage of the ions in seawater and obtain high-value-added products. In this way, photocatalytic seawater splitting can be effectively developed.

We believe that in the near future, after in-depth system research and continuous optimization of material and systems, the research on H_2 production by photocatalytic seawater splitting will make great progress.

Acknowledgements

This work was supported by the National Natural Science Foundation of China (Nos. 21703046 and 21972028), the Strategic Priority Research Program of Chinese Academy of Science (No. XDB36000000) and the Ministry of Science and Technology of China (No. 2016YFF0203803).

References

[1] Ahmad, H.; Kamarudin, S. K.; Minggu, L. J.; Kassim, M. Hydrogen from photo-catalytic water splitting process: A review. *Renew. Sustain. Energy Rev.* **2015**, *43*, 599–610.

[2] Dubey, P. K.; Tripathi, P.; Tiwari, R. S.; Sinha, A. S. K.; Srivastava, O. N. Synthesis of reduced graphene oxide-TiO_2 nanoparticle composite systems and its application in hydrogen production. *Int. J. Hydrogen Energy* **2014**, *39*, 16282–16292.

[3] Moriya, Y.; Takata, T.; Domen, K. Recent progress in the development of (oxy) nitride photocatalysts for water splitting under visible-light irradiation. *Coord. Chem. Rev.* **2013**, *257*, 1957–1969.

[4] Osterloh, F. E. Inorganic nanostructures for photoelectrochemical and photocatalytic water splitting. *Chem. Soc. Rev.* **2013**, *42*, 2294–2320.

[5] Xing, J.; Fang, W. Q.; Zhao, H. J.; Yang, H. G. Inorganic photocatalysts for overall water splitting. *Chem. —Asian J.* **2012**, *7*, 642–657.

[6] Chen, X. B.; Shen, S. H.; Guo, L. J.; Mao, S. S. Semiconductor-based photocatalytic hydrogen generation. *Chem. Rev.* **2010**, *110*, 6503–6570.

[7] Maeda, K.; Domen, K. Photocatalytic water splitting: Recent progress and future challenges. *J. Phys. Chem. Lett.* **2010**, *1*, 2655–2661.

[8] Maeda, K.; Domen, K. New non-oxide photocatalysts designed for overall water splitting under visible light. *J. Phys. Chem. C* **2007**, *111*, 7851–7861.

[9] Lewis, N. S. Toward cost-effective solar energy use. *Science* **2007**, *315*, 798–801.

[10] Cai, J. S.; Shen, J. L.; Zhang, X. N.; Ng, Y. H.; Hang, J. Y.; Guo, W. X.; Lin, C. J.; Lai, Y. K. Light-driven sustainable hydrogen production utilizing TiO_2 nanostructures: A review. *Small Methods* **2019**, *3*, 1800184.

[11] Fang, S. Y.; Hu, Y. H. Recent progress in photocatalysts for overall water splitting. *Int. J. Energy Res.* **2019**, *43*, 1082–1098.

[12] Chen, S. S; Takata, T.; Domen, K. Particulate photocatalysts for overall water splitting. *Nat. Rev. Mater.* **2017**, *2*, 17050.

[13] Muradov, N. Z.; Veziroğlu, T. N. "Green" path from fossil-based to hydrogen economy: An overview of carbon-neutral technologies. *Int. J. Hydrogen Energy* **2008**, *33*, 6804–6839.

[14] Pinaud, B. A.; Benck, J. D.; Seitz, L. C.; Forman, A. J.; Chen, Z. B.; Deutsch, T. G.; James, B. D.; Baum, K. N.; Baum, G. N.; Ardo, S. et al. Technical and economic feasibility of centralized facilities for solar hydrogen production via photocatalysis and photoelectrochemistry. *Energy Environ. Sci.* **2013**, *6*, 1983–2002.

[15] Xu, P. T.; Mccool, N. S.; Mallouk, T. E. Water splitting dye-sensitized solar cells. *Nano Today* **2017**, *14*, 42–58.

[16] Zhang, W.; Qi, J.; Liu, K. Q.; Cao, R. A nickel-based integrated electrode from an autologous growth strategy for highly efficient water oxidation. *Adv. Energy Mater.* **2016**, *6*, 1502489.

[17] Maeda, K. Photocatalytic water splitting using semiconductor particles: History and recent developments. *J. Photochem. Photobiol., C: Photochem. Rev.* **2011**, *12*, 237–268.

[18] Walter, M. G.; Warren, E. L.; McKone, J. R.; Boettcher, S. W.; Mi, Q. X.; Santori, E. A.; Lewis, N. S. Solar water splitting cells. *Chem. Rev.* **2010**, *110*, 6446–6473.

[19] Luo, J. S.; Im, J. H.; Mayer, M. T.; Schreier, M.; Nazeeruddin, M. K.; Park, N. G.; Tilley, S. D.; Fan, H. J.; Grätzel, M. Water photolysis at 12.3% efficiency via perovskite photovoltaics and Earth-abundant catalysts. *Science* **2014**, *345*, 1593–1596.

[20] Liu, X. L.; Ma, R.; Wang, X. X.; Ma, Y.; Yang, Y. P.; Zhuang, L.; Zhang, S.; Jehan, R.; Chen, J. R.; Wang, X. K. Graphene oxide-based materials for efficient removal of heavy metal ions from aqueous solution: A review. *Environ. Pollut.* **2019**, *252*, 62–73.

[21] Chini, C. M.; Schreiber, K. L.; Barker, Z. A.; Stillwell, A. S. Quantifying energy and water savings in the U.S. residential sector. *Environ. Sci. Technol.* **2016**, *50*, 9003–9012.

[22] Schwarzenbach, R. P.; Escher, B. I.; Fenner, K.; Hofstetter, T. B.; John, C. A.; Von Gunten, U.; Wehrli, B. The challenge of micropollutants in aquatic systems. *Science* **2006**, *313*, 1072–1077.

[23] Vörösmarty, C. J.; Green, P.; Salisbury, J.; Lammers, R. B. Global water resources: Vulnerability from climate change and population growth. *Science* **2000**, *289*, 284–288.

[24] Fukuzumi, S.; Lee, Y. M.; Nam, W. Fuel production from seawater and fuel cells using seawater. *ChemSusChem.* **2017**, *10*, 4264–4276.

[25] Kumaravel, V.; Abdel-Wahab, A. A short review on hydrogen, biofuel, and electricity production using seawater as a medium. *Energy Fuels* **2018**, *32*, 6423–6437.

[26] Ichikawa, S. Photoelectrocatalytic production of hydrogen from natural seawater under sunlight. *Int. J. Hydrogen Energy* **1997**, *22*, 675–678.

[27] Ji, S. M.; Jun, H.; Jang, J. S.; Son, H. C.; Borse, P. H.; Lee, J. S. Photocatalytic hydrogen production from natural seawater. *J. Photochem. Photobiol., A: Chem.* **2007**, *189*, 141–144.

[28] Li, L. Y.; Zhou, Z. M.; Li, L. Y.; Zhuang, Z. Y.; Bi, J. H.; Chen, J. H.; Yu, Y.; Yu, J. H. Thioether-functionalized 2D covalent organic framework featuring specific affinity to Au for photocatalytic hydrogen production from seawater. *ACS Sustainable Chem. Eng.* **2019**, *7*, 18574–18581.

[29] Li, Y. X.; He, F.; Peng, S. Q.; Lu, G. X.; Li, S. B. Photocatalytic H_2 evolution from NaCl saltwater over $ZnS_{1-x-0.5y}O_x(OH)_y$-ZnO under visible light irradiation. *Int. J. Hydrogen Energy* **2011**, *36*, 10565–10573.

[30] Li, Y. X.; Lin, S. Y.; Peng, S. Q.; Lu, G. X.; Li, S. B. Modification of $ZnS_{1-x-0.5y}O_x(OH)_y$-ZnO photocatalyst with NiS for enhanced visible-light-driven hydrogen generation from seawater. *Int. J. Hydrogen Energy* **2013**, *38*, 15976–15984.

[31] Li, Z. S.; Luo, W. J.; Zhang, M. L.; Feng, J. Y.; Zou, Z. G. Photoelectrochemical cells for solar hydrogen production: Current state of promising photoelectrodes, methods to improve their properties, and outlook. *Energy Environ. Sci.* **2013**, *6*, 347–370.

[32] Luo, W. J; Yang, Z. S.; Li, Z. S.; Zhang, J. Y.; Liu, J. G.; Zhao, Z. Y.; Wang, Z. Q.; Yan, S. C.; Yu, T.; Zou, Z. G. Solar hydrogen generation from seawater with a modified $BiVO_4$ photoanode. *Energy Environ. Sci.* **2011**, *4*, 4046–4051.

[33] Ran, J. R.; Zhang, J.; Yu, J. G.; Jaroniec, M.; Qiao, S. Z. Earth-abundant cocatalysts for semiconductor-based photocatalytic water splitting. *Chem. Soc. Rev.* **2014**, *43*, 7787–7812.

[34] Fajrina, N.; Tahir, M. A critical review in strategies to improve photocatalytic water splitting towards hydrogen production. *Int. J. Hydrogen Energy* **2019**, *44*, 540–577.

[35] Moniz, S. J. A.; Shevlin, S. A.; Martin, D. J.; Guo, Z. X.; Tang, J. W. Visible-light driven heterojunction photocatalysts for water splitting —A critical review. *Energy Environ. Sci.* **2015**, *8*, 731–759.

[36] Hisatomi, T.; Domen, K. Reaction systems for solar hydrogen production via water splitting with particulate semiconductor photocatalysts. *Nat. Catal.* **2019**, *2*, 387–399.

[37] Miseki, Y.; Sayama, K. Photocatalytic water splitting for solar hydrogen production using the carbonate effect and the Z-scheme reaction. *Adv. Energy Mater.* **2019**, *9*, 1801294.

[38] Wang, Y. O.; Suzuki, H.; Xie, J. J.; Tomita, O.; Martin, D. J.; Higashi, M.; Kong, D.; Abe, R.; Tang, J. W. Mimicking natural photosynthesis: Solar to renewable H_2 fuel synthesis by Z-scheme water splitting systems. *Chem. Rev.* **2018**, *118*, 5201–5241.

[39] Guan, X. J.; Chowdhury, F. A.; Pant, N.; Guo, L. J.; Vayssieres, L.; Mi, Z. T. Efficient unassisted overall photocatalytic seawater splitting on GaN-based nanowire arrays. *J. Phys. Chem. C* **2018**, *122*, 13797–13802.

[40] Wu, M. C.; Sápi, A.; Avila, A.; Szabó, M.; Hiltunen, J.; Huuhtanen, M.; Tóth, G.; Kukovecz, Á.; Kónya, Z.; Keiski, R. et al. Enhanced

photocatalytic activity of TiO_2 nanofibers and their flexible composite films: Decomposition of organic dyes and efficient H_2 generation from ethanol-water mixtures. *Nano Res*. **2011**, *4*, 360–369.

[41] Li, R. G.; Weng, Y. X.; Zhou, X.; Wang, X. L.; Mi, Y.; Chong, R. F.; Han, H. X.; Li, C. Achieving overall water splitting using titanium dioxide-based photocatalysts of different phases. *Energy Environ. Sci*. **2015**, *8*, 2377–2382.

[42] Peng, S. Q.; Liu, X. Y.; Ding, M.; Li Y. X. Preparation of CdS-Pt/TiO_2 composite and the properties for splitting sea water into hydrogen under visible light irradiation. *J. Mol. Catal*. **2013**, *27*, 459–466.

[43] Gao, M. M.; Connor, P. K. N.; Ho, G. W. Plasmonic photothermic directed broadband sunlight harnessing for seawater catalysis and desalination. *Energy Environ. Sci*. **2016**, *9*, 3151–3160.

[44] Simamora, A. J.; Hsiung, T. L.; Chang, F. C.; Yang, T. C.; Liao, C. Y.; Wang, H. P. Photocatalytic splitting of seawater and degradation of methylene blue on CuO/nano TiO_2. *Int. J. Hydrogen Energy* **2012**, *37*, 13855–13858.

[45] Sinhamahapatra, A.; Lee, H. Y.; Shen, S. H.; Mao, S. S.; Yu, J. S. H-doped TiO_{2-x} prepared with MgH_2 for highly efficient solar-driven hydrogen production. *Appl. Catal. B: Environ*. **2018**, *237*, 613–621.

[46] Simamora, A. J.; Chang, F. C.; Wang, H. P.; Yang, T. C.; Wei, Y. L.; Lin, W. K. H_2 fuels from photocatalytic splitting of seawater affected by nano-TiO_2 promoted with CuO and NiO. *Int. J. Photoenergy* **2013**, *2013*, 419182.

[47] DeepanPrakash, D.; Premnath, V.; Raghu, C.; Vishnukumar, S.; Jayanthi, S. S.; Easwaramoorthy, D. Harnessing power from sea water using nano material as photocatalyst and solar energy as light source: The role of hydrocarbon as dual agent. *Int. J. Energy Res*. **2014**, *38*, 249–253.

[48] Song, T.; Zhang, P. Y.; Wang, T. T.; Ali, A.; Zeng, H. P. Constructing a novel strategy for controllable synthesis of corrosion resistant Ti^{3+} self-doped titanium-silicon materials with efficient hydrogen evolution activity from simulated seawater. *Nanoscale* **2018**, *10*, 2275–2284.

[49] Wang, C.; Abdul-Rahman, H.; Rao, S. P. A new design of luminescent solar concentrator and its trial run. *Int. J. Energy Res*. **2010**, *34*, 1372–1385.

[50] Cao, S.; Chan, T. S.; Lu, Y. R.; Shi, X. H.; Fu, B.; Wu, Z. J.; Li H. M.; Liu, K.; Alzuabi, S.; Cheng, P. et al. Photocatalytic pure water splitting with high efficiency and value by Pt/porous brookite TiO_2 nanoflutes. *Nano Energy* **2020**, *67*, 104287.

[51] Sakurai, H.; Kiuchi, M.; Jin, T. Pt/TiO_2 granular photocatalysts for hydrogen production from aqueous glycerol solution: Durability against seawater constituents and dissolved oxygen. *Catal. Commun*. **2018**, *114*, 124–128.

[52] Speltini, A.; Scalabrini, A.; Maraschi, F.; Sturin, M.; Pisanu, A.; Malavasi, L.; Profumo, A. Improved photocatalytic H_2 production assisted by aqueous glucose biomass by oxidized g-C_3N_4. *Int. J. Hydrogen Energy* **2018**, *43*, 14925–14933.

[53] Yang, C. W.; Qin, J. Q.; Rajendran, S.; Zhang, X. Y.; Liu, R. P. WS_2 and C-TiO_2 nanorods acting as effective charge separators on g-C_3N_4 to boost visible-light activated hydrogen production from seawater. *ChemSusChem* **2018**, *11*, 4077–4085.

[54] Mishra, B.; Mishra, S.; Satpati B.; Chaudhary, Y. S. Engineering the surface of a polymeric photocatalyst for stable solar-to-chemical fuel conversion from seawater. *ChemSusChem* **2019**, *12*, 3383–3389.

[55] Abe, R.; Higashi, M.; Sayama, K.; Abe, Y.; Sugihara, H. Photocatalytic activity of R_3MO_7 and $R_2Ti_2O_7$ (R = Y, Gd, La; M = Nb, Ta) for water splitting into H_2 and O_2. *J. Phys. Chem. B* **2006**, *110*, 2219–2226.

[56] Yang, T. C.; Chang, F. C.; Wang, H. P.; Wei, Y. L.; Jou, C. J. Photocatalytic splitting of seawater effected by (Ni-ZnO)@C nanoreactors. *Mar. Pollut. Bull*. **2014**, *85*, 696–699.

[57] Cui, G. W.; Wang, W.; Ma, M. Y.; Xie, J. F.; Shi, X. F.; Deng, N.; Xin, J. P.; Tang, B. IR-Driven photocatalytic water splitting with WO_2-Na_xWO_3 hybrid conductor material. *Nano Lett*. **2015**, *15*, 7199–7203.

[58] Qiu, B. C.; Zhu, Q. H.; Xing, M. Y.; Zhang, J. L. A robust and efficient catalyst of $Cd_xZn_{1-x}Se$ motivated by CoP for photocatalytic hydrogen evolution under sunlight irradiation. *Chem. Commun*. **2017**, *53*, 897–900.

[59] Yang, X. Y.; Hu, Z. C.; Yin, Q. W.; Shu, C.; Jiang, X. F.; Zhang, J.; Wang, X. H.; Jiang, J. X.; Huang, F.; Cao, Y. Water-soluble conjugated molecule for solar-driven hydrogen evolution from salt water. *Adv. Funct. Mater*. **2019**, *29*, 1808156.

[60] Liu, Y. Y.; Liao, Z. J.; Ma, X. L.; Xiang, Z. H. Ultrastable and efficient visible-light-driven hydrogen production based on donor-acceptor copolymerized covalent organic polymer. *ACS Appl. Mater. Interfaces* **2018**, *10*, 30698–30705.

[61] Liu, Y. Y.; Xiang, Z. H. Fully conjugated covalent organic polymer with carbon-encapsulated Ni_2P for highly sustained photocatalytic H_2 production from seawater. *ACS Appl. Mater. Interfaces* **2019**, *11*, 41313–41320.

[62] Zhu, C.; Liu, C. A.; Fu, Y. J.; Gao, J.; Huang, H.; Liu, Y.; Kang, Z. H. Construction of CDs/CdS photocatalysts for stable and efficient hydrogen production in water and seawater. *Appl. Catal. B: Environ*. **2019**, *242*, 178–185.

[63] Li, Y. X.; He, F.; Peng, S. Q.; Gao, D.; Lu, G. X.; Li, S. B. Effects of electrolyte NaCl on photocatalytic hydrogen evolution in the presence of electron donors over Pt/TiO_2. *J. Mol. Catal. A: Chem*. **2011**, *341*, 71–76.

[64] Maeda, K.; Masuda, H.; Domen, K. Effect of electrolyte addition on activity of $(Ga_{1-x}Zn_x)(N_{1-x}O_x)$ photocatalyst for overall water splitting under visible light. *Catal. Today* **2009**, *147*, 173–178.

[65] Li, Y. X.; Gao, D.; Peng, S. Q.; Lu, G. X.; Li, S. B. Photocatalytic hydrogen evolution over Pt/$Cd_{0.5}Zn_{0.5}S$ from saltwater using glucose as electron donor: An investigation of the influence of electrolyte NaCl. *Int. J. Hydrogen Energy* **2011**, *36*, 4291–4297.

[66] Li, Y. X.; Lu, G. X.; Li, S. B. Photocatalytic hydrogen generation and decomposition of oxalic acid over platinized TiO_2. *Appl. Catal. A: Gen*. **2001**, *214*, 179–185.

[67] Krivec, M.; Dillert, R.; Bahnemann, D. W.; Mehle, A.; Štrancar, J.; Dražić, G. The nature of chlorine-inhibition of photocatalytic degradation of dichloroacetic acid in a TiO_2-based microreactor. *Phys. Chem. Chem. Phys*. **2014**, *16*, 14867–14873.